Contribution of inflammation and fat infiltration to T2

THESIS

submitted in partial fulfillment of the
requirements for the degree of

BACHELOR OF SCIENCE
in
PHYSICS

Author :	A. M. Vlaar
Student ID :	s 1535013
Supervisor :	J. W. M. Beenakker
2^{nd} corrector :	T. H. Oosterkamp

Leiden, The Netherlands, January 23, 2018

Contribution of inflammation and fat infiltration to T2

A. M. Vlaar

Huygens-Kamerlingh Onnes Laboratory, Leiden University
P.O. Box 9500, 2300 RA Leiden, The Netherlands

January 23, 2018

Abstract

The MRI time constant T2 of water is an indication of inflammation in muscles but is difficult to identify when fat is infiltrated in the muscle. A model that takes both the T2 of fat and the T2 of water into account can be used to determine the T2 of water when the T2 of fat is known. The T2 of fat in affected muscles is equal to subcutaneous fat. To determine the T2 of subcutaneous fat the Extended Phase Graph model is used which calculates the contribution of spins to the MRI signal taking the effects of relaxation, dephasing and radiofrequency pulses into account. It is therefore able to keep track of the contribution of stimulated echoes to the MRI signal. The observed T2 fat values show differences in the order of magnitude of 10 ms in different parts of subcutaneous fat. T2 fat values determined by the presented EPG model are 50 to 80 ms higher than the actual values. Suggested improvements to the EPG model includes usages of a different shaped RF pulse and to take into account different gradient strengths, frequencies of spins and the chemical shift of water and fat.

Contents

Chapter 1

Introduction

The weak muscles of patients with muscular dystrophy diseases often suffer from inflammation. If not treated effectively, the inflammation leads to the replacement of muscle tissue by fat [1] which is irreversible [2]. Examples of follow-up methods, to determine if the inflammation inhibitors are successful, are the distance that the patient can walk in 6 minutes, the time it takes the patient to stand up or the maximum force that can be performed [3] and depend on the effort and motivation of the patient. An invasive method to measure progression is by taking a biopsy of the muscle. Magnetic resonance imaging (MRI), however, can determine the time constant T2 of water in muscles, which increases when inflammation is present [4]. Therefore MRI can be used as a quantitative non-invasive follow-up method.

1.1 Magnetic Resonance Imaging

In order to understand the time constant T2, the basic concept of MRI will be explained.

The nuclei of hydrogen atoms (protons) have a positive charge which rotates about its axis. Due to this property these protons have a magnetic moment (μ). Without any external magnetic field, the direction of μ is randomly distributed. The MRI scanner consists of a strong magnet that produces a static magnetic field (B_0) in the z-direction of the MRI-coordinate system. The z component of μ is parallel or anti-parallel to this magnetic field and as a result the magnitude of the magnetic moment is positioned in an angle of 54.7°relative to B_0 [5]. The MRI scanner can detect a signal only from the difference in the number of protons in the parallel and anti-

parallel state. Since the parallel state is associated with lower energy, there will be more protons in this state. At room temperature and at 3 Tesla, of 1 million protons, there are 10 more in the parallel state than in the anti-parallel state [5]. Which means that of every million protons 10 protons produce a signal.

1.1.1 MR signal

Since the magnetic moment is positioned at an angle of 54.7°and precessing around B_0 the net magnetization in the x- and y-direction is cancelled out. With more protons in the parallel state, a net magnetization (M_0) in the positive z-direction remains.

An electromagnetic pulse (radio frequency or RF pulse) can tip M_0 into the xy-plane. Faraday's law states that a changing magnetic field can induce a current. Since the magnetization vector is rotating in the xy-plane the magnetic field it produces is changing and can induce a current which is the MR signal.

1.1.2 Larmor frequency

Because μ is positioned at an angle of 54.7°relative to B_0, a torque is created since both magnetic vectors want to align. Due to this torque, μ starts to precess around B_0. The rate with which it precesses is called the Larmor frequency and defined as:

$$\omega = \gamma B_0 \tag{1.1}$$

Where ω is the Larmor frequency and γ is the gyromagnetic ratio between the magnetic moment and the angular momentum of a particle. The Larmor frequency at 3 Tesla of protons is 128 MHz [5].

1.1.3 Imaging

In order to create an image, the MR signal needs to be localized. Equation 1.1 shows that the frequency of the protons depends on the magnetic field they experience. When an additional magnetic field is applied where the strength depends on the location (a magnetic gradient) the Larmor frequency of the protons depends on their location.

Relaxation

The magnitude of the magnetization vector in the xy-plane will decay by two independent processes. Firstly M_0 will align back along the z-axis, back to equilibrium. This type of decay is called T1 relaxation and is coupled to a specific time constant T1 [6]. The second process is called T2 relaxation, this is the decay of the net magnetization in the xy-plane. After the RF pulse has been applied all the spins have the same phase with respect to y' axis in the rotating frame of reference. Hydrogen atoms interact with nearby hydrogen atoms of the same molecule, which is called J-coupling [7]. This causes the spins to rotate at slightly different frequencies. As a result, the phases of these spins with respect to y' will differ more in time, this process is known as dephasing [5]. Due to this dephasing, the net magnetization in the xy-plane will decay. The time constant related to this type of relaxation is T2. Dephasing is not only caused by interaction between spins but also by local B_0 field inhomogeneity. The two main causes of this inhomogeneity are the fact that it not possible to construct a perfect magnet but mostly because the magnetic susceptibility is not the same for all biological tissues [5]. The relaxation caused by B_0 field inhomogeneity is called $T2^+$. T1 and T2 values at 3 Tesla of subcutaneous fat and muscle tissue are stated in table 1.1, for inflamed muscle the T2 value is higher than 30 ms.

Table 1.1: *Values for T1 and T2 in ms of different tissues at 3 Tesla [5].*

	T1	**T2**
Subcutaneous fat	360	130
muscle tissue	1420	30

Spin echo sequences

A 90°RF pulses tips the net magnetization into the xy-plane and spins dephase due to T2 and $T2^+$. At time interval $t = n * \tau + \tau/2$, $n \in$ [0,1, ... n], 180°RF pulses are applied causing the spins to rephase at $t = n * \tau + \tau$ on the -y' axis, when the MR signal intensity is measured. Therefore the 180°RF pulses cancel the effect of $T2^+$ and due to this sequence the MRI signal depends ideally only on T1 and T2.

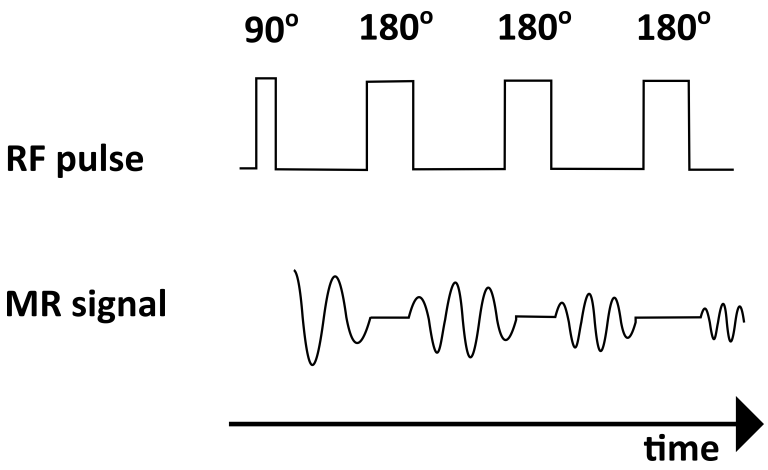

Figure 1.1: *The 90° RF pulse tips the net magnetization into the xy-plane causing the maximum intensity which dephases. Due to the subsequent 180° pulses the spins rephase again and form an echo. At the mid of each echo the MRI signal is measured.*

1.1.4 Measurement of a muscle

The MR signal of a affected muscle that contains fatty tissue due to fat infiltration, is composed of the signal from fat and the signal of muscle. The protons in muscle that produce the MR signal are mostly from water molecules. Therefore the signal from muscle is commonly referred to as water signal. T2 of water is a potential biomarker since it increases when inflammation is present. The T2 of the measured signal is a combination of T2 of fat and the T2 of water. To measure the water T2, the signal from fat needs to be separated from the water signal.

Magnetic Resonance spectroscopy

The magnetic field that electrons produce is opposite to B_0 [5] and therefore reduces the magnetic field around the spin. This shielding effect varies among protons of different molecules. The oxygen atom of a water molecule attracts the electrons of the hydrogen atom more than the carbon atom of a fat molecule. Therefor the Larmor frequency of water is slightly higher (400 Hz, at 3 Tesla) than the frequency of fat [5]. MR-spectroscopy is based on these differences and can be used to determine the T2 value of fat and water separately. Unfortunately, it is a time-consuming method and is therefore not applicable in a clinical setting.

Bi-exponential fit

The MRI signal could be modelled with a bi-exponential fit (equation 1.1.4)

$$S = f * e^{-t/T2_{fat}} + w * e^{-t/T2_{water}} \tag{1.2}$$

Where S is the MRI signal, f and w are the amplitude of the fat and water signal respectively and $T2_{fat}$ and $T2_{water}$ are both T2 values. The T2 value of subcutaneous fat is assumed to be equal to the T2 value of infiltrated fat in the muscle [4]. To reduce the number of unknown parameters, $T2_{fat}$ is determined with an exponential fit on subcutaneous fat assuming there is no water present in subcutaneous fat. Subsequently, this T2 value can be used as a fixed parameter to fit fat infiltrated muscle and determine the T2 value of water. Figure 1.2 shows the exponential fit on a subcutaneous fat voxel. The measurement points do not follow a perfect exponential decay, therefore, the first measurement point is left out. That suggests that some factor is not taking into account.

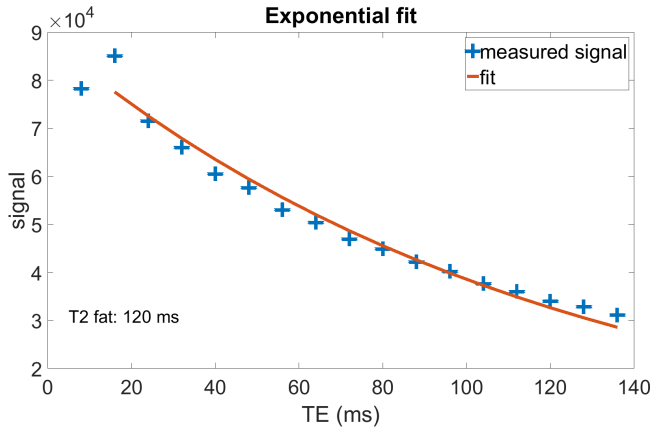

Figure 1.2: *The MRI signal of subcutaneous fat. An exponential fit is preformed and the first measurement point is left out.*

Tri-exponential fit

The shielding effect mentioned in 1.1.4 is not the same for all hydrogen atoms in fat [8]. As a result, parts of fat resonate at different frequencies. Figure 1.3 shows the triglyceride molecule where the colours identify the hydrogen atoms that resonate at the same frequency. The corresponding coloured peaks are represented by their chemical shift in ppm. Since the MRI signal of fat consists of multiple peaks, the T2 value of fat could consist of multiple values as well. To find these T2 values a bi-exponential fit

was performed on subcutaneous fat [4] assuming that the T2 of fat could be described by a long and a short T2 value. A tri-exponential fit was performed on an affected muscle with the determined T2 values as fixed parameters in order to determine $T2_{water}$. The determined $T2_{fat}$ values where 440 ms and 80 ms, while the T2 values of different fat peaks are in the range of 40 - 80 ms [4]. Although the performed fit is better than the mono-exponential fit, the argumentation for this approach is not sufficient.

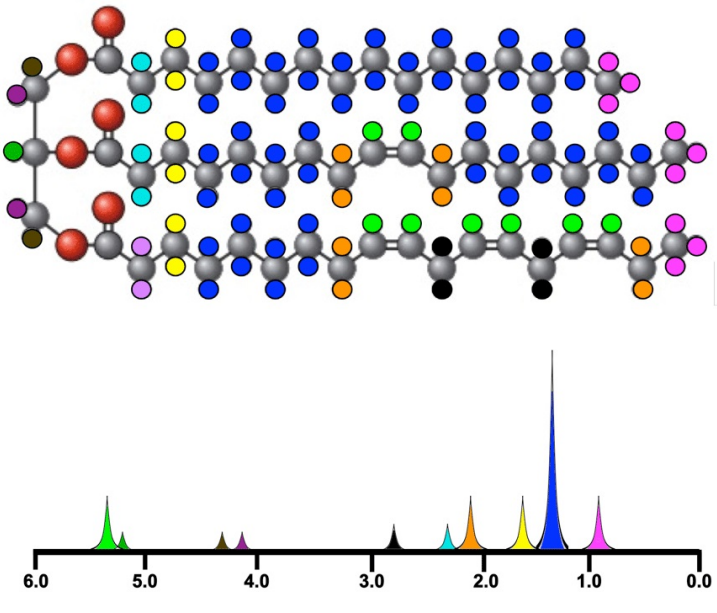

Figure 1.3: *Triglyceride molecule, the coloured hydrogen atoms correspond to the resonant peaks expressed in ppm.[8]*

Extended phase graph

Both exponential models only taking into account that the MRI signal is decaying because of T2 relaxation, in reality, however, the spins are affected by gradients that are turned on and off, RF pulses that are applied and the relaxation (both T1 and T2) that takes place during the measurements. The extended phase graph algorithm calculates the reaction of the spins to these events [9], therefore at each measurement point in time, the intensity of the MRI signal can be determined.

Chapter 2

Methodology

The code used in this project was written in Matlab [10] and based on the EPG format provided by Weigel in 2015 following the guidelines of the corresponding article [9].

2.1 Basic concept of Extended phase graph

The EPG model describes a group of spins by their phase. The effects of RF pulses, gradients and relaxation can be described by matrix multiplications with the spin states.

2.1.1 Phase graph

The net magnetization of each group of spins that rotate at the same frequency can be described by their orientation in x, y and z. The net magnetization can, therefore, be described as a vector (equation 2.1).

$$\begin{bmatrix} M_x \\ M_y \\ M_z \end{bmatrix} \tag{2.1}$$

By changing the basis from the real to the complex plane, 180° RF pulses can be described by a simple complex conjugate operation: (M_+)*=M_-, with:

$$M_+ = M_x + iM_y \tag{2.2}$$
$$M_- = M_x - iM_y \tag{2.3}$$

The sum of the group of spins along the gradient direction represents the total net magnetization [9], this is equal to the Fourier decomposition of M_+ (equation 2.4).

$$\tilde{F}_+(k) = \int_V M_+(r) e^{-ikr} d^3r \tag{2.4}$$

Where k is the wave vector and V is a macroscopically large sample volume. Only the group of spins with k = 0 contribute to the signal since $k \neq 0$ represents the group of spins that are dephased [9].

2.1.2 Effect of an RF pulse

The effect of an arbitrary RF pulse on a group of spins can be described by a matrix operation on the complex magnetization vector.

$$\begin{bmatrix} M_+ \\ M_- \\ M_z \end{bmatrix}^+ = \begin{bmatrix} cos^2\frac{\alpha}{2} & e^{2i\Phi}sin^2\frac{\alpha}{2} & -ie^{i\Phi}sin\alpha \\ e^{-2i\Phi}sin^2\frac{\alpha}{2} & cos^2\frac{\alpha}{2} & ie^{-i\Phi}sin\alpha \\ -\frac{i}{2}e^{-i\Phi}sin\alpha & \frac{i}{2}e^{i\Phi}sin\alpha & cos\alpha \end{bmatrix} \cdot \begin{bmatrix} M_+ \\ M_- \\ M_z \end{bmatrix}^- \tag{2.5}$$

Where α is the flip angle around Φ, Φ is the RF phase angle with respect to the x-axis. The - and + sign are indicators of before and after the RF pulse respectively.

Each RF pulse will split all present components into three new components [11] of which the amplitude depends on the flip angle α [9].

2.1.3 Extended phase graph

Equation 2.5 describes the effect of a RF pulse to a group of spins, contrary with the Fourier representation of the magnetization which describe a whole ensemble of a group of spins over time. To have a complete description of the MRI signal, the extended phase graph algorithm combines the partitioning effect with the Fourier representation of magnetization [9].

$$\tilde{F}_+(k) = \int_V M_+(r) e^{-ikr} d^3r \tag{2.6}$$

$$\tilde{F}_-(k) = \int_V M_-(r) e^{-ikr} d^3r \tag{2.7}$$

$$\tilde{Z}(k) = \int_V M_z(r) e^{-ikr} d^3r \tag{2.8}$$

The states with k = 0 represents echoes, where:

$$\tilde{F}_+(0) = (\tilde{F}_-(0))^* \tag{2.9}$$

with * is the complex conjugate operator. The rotation matrix in equation 2.5 does not depend on k, with the change of basis from complex to Fourier space, this rotation matrix does not change. Because the value of $\tilde{F}$ depends on k and on time, the notation changes to:

$$\tilde{F}_k(t) \tag{2.10}$$

The magnetization at time t can be describe by:

$$\begin{bmatrix} \tilde{F}_0(t) & \tilde{F}_1(t) & \tilde{F}_2(t) & ... & \tilde{F}_k(t) \\ \tilde{F}_0^*(t) & \tilde{F}_{-1}^*(t) & \tilde{F}_{-2}^*(t) & ... & \tilde{F}_{-k}^*(t) \\ \tilde{Z}_0(t) & \tilde{Z}_1(t) & \tilde{Z}_2(t) & ... & \tilde{Z}_k(t) \end{bmatrix} \tag{2.11}$$

A 90°RF pulse around the y-axis tips the magnetization onto the x-axis, creating the following state:

$$\begin{bmatrix} 1 & 0 & 0 & ... \\ 1 & 0 & 0 & ... \\ 0 & 0 & 0 & ... \end{bmatrix} \tag{2.12}$$

Dephasing due to gradients will shift each component with +k, except for the states in Z which do not shift in phase.

$$\begin{bmatrix} 0 & 1 & 0 & ... \\ 0 & 0 & 0 & ... \\ 0 & 0 & 0 & ... \end{bmatrix} \tag{2.13}$$

The magnetization described by $\tilde{F}_k(t)$ shift to the right and its value of k will only increase, therefore they describe the magnetization that dephases. $\tilde{F}_{-k}^*(t)$ shifts to the left and can end on the position of $\tilde{F}_0^*(t)$ which contributes to the signal and therefore represents the magnetization that rephases.

Disregarding relaxation, a 180°pulse flips all transverse magnetization.

$$\begin{bmatrix} 0 & 0 & 0 & ... \\ 0 & 1 & 0 & ... \\ 0 & 0 & 0 & ... \end{bmatrix} \tag{2.14}$$

After the RF pulse the magnetization will dephase again:

$$\begin{bmatrix} 1 & 0 & 0 & ... \\ 1 & 0 & 0 & ... \\ 0 & 0 & 0 & ... \end{bmatrix} \tag{2.15}$$

As a result, an echo is formed with the maximum intensity since relaxation was disregarded and only 90°and 180°pulses where used.

2.2 Modeling MRI signal

The EPG code provided by Weigel could already handle different values of refocusing pulses, but the excitation pulse was fixed at 90°. There are many factors influencing the actual flip angle of the RF pulse, for example, the pulse profile, slice select gradients and B_0 field inhomogeneities [12]. Causes the RF pulses to be different than 90°or 180°. As this has an effect on the accuracy of the EPG fit, the original code was improved to handle different value of the RF pulse.

2.2.1 EPG model

The known parameters that are necessary to determine the intensity of the MRI signal are the times at which echoes occur (TEs), the excitation flip angle $(alpha\_ex)$, the refocusing flip angle $(alpha\_in)$, T1 and T2.
The Turbo Spin Echo (TSE) sequence was used in these measurements together with the CPMG technique: the 90°RF pulse rotates the magnetization around the y-axis and is followed by several 180°pulses that rotate the magnetization around the x-axis.

Due to an arbitrary excitation pulse α, spins end up in the following state:

$$\tilde{F}_0(t_0) = sin(\alpha) \tag{2.16}$$

$$\tilde{F}_0^*(t_0) = sin(\alpha) \tag{2.17}$$

$$\tilde{Z}_0(t_0) = cos(\alpha) \tag{2.18}$$

With τ the time between two RF pulses. In the time between t = 0 and t = $\tau/2$ the magnetization has experienced relaxation and dephasing. T2 relaxation can be describe by equations 2.19 - 2.20 [9].

For all k:

$$\tilde{F}_k(t_{\frac{1}{2}}) = e^{(-\tau/2/T2)} * \tilde{F}_k(t_0) \tag{2.19}$$

$$\tilde{F}_k^*(t_{\frac{1}{2}}) = e^{(-\tau/2/T2)} * \tilde{F}_k^*(t_0) \tag{2.20}$$

T1 relaxation is described by equations 2.21 - 2.22 [9].

for k = 0

$$\tilde{Z}_k(t_{\frac{1}{2}}) = e^{(-\tau/2/T1)} * \tilde{Z}_k(t_0) + 1 - e^{(-\tau/2/T1)} \tag{2.21}$$

for k > 0

$$\tilde{Z}_k(t_{\frac{1}{2}}) = e^{(-\tau/2/T1)} * \tilde{Z}_k(t_0) \tag{2.22}$$

Since Z is real equation 2.23 holds for longitudinal magnetization therefore k < 0 can be disregarded.

$$\tilde{Z}(-k) = (\tilde{Z}(k))^* = \tilde{Z}(k) \tag{2.23}$$

Dephasing is describe by a change of k, where ΔK = 1, because the sequence is periodic and the relaxation and rotation matrices do not depend on k [9]. If the current transverse magnetization is represented by:

$$\begin{bmatrix} \tilde{F}_0(t_{\frac{1}{2}}) & \tilde{F}_1(t_{\frac{1}{2}}) & \tilde{F}_2(t_{\frac{1}{2}}) & \tilde{F}_3(t_{\frac{1}{2}}) & ... & \tilde{F}_k(t_{\frac{1}{2}}) \\ \tilde{F}_0^*(t_{\frac{1}{2}}) & \tilde{F}_{-1}^*(t_{\frac{1}{2}}) & \tilde{F}_{-2}^*(t_{\frac{1}{2}}) & \tilde{F}_{-3}^*(t_{\frac{1}{2}}) & ... & \tilde{F}_k^*(t_{\frac{1}{2}}) \end{bmatrix} \tag{2.24}$$

Then after dephasing the states are shifted as in equation 2.25.

$$\begin{bmatrix} \tilde{F}_{-1}(t_{\frac{1}{2}}) & \tilde{F}_0(t_{\frac{1}{2}}) & \tilde{F}_1(t_{\frac{1}{2}}) & \tilde{F}_2(t_{\frac{1}{2}}) & ... & \tilde{F}_{k-1}(t_{\frac{1}{2}}) \\ \tilde{F}_{-1}^*(t_{\frac{1}{2}}) & \tilde{F}_{-2}^*(t_{\frac{1}{2}}) & \tilde{F}_{-3}^*(t_{\frac{1}{2}}) & \tilde{F}_{-4}^*(t_{\frac{1}{2}}) & ... & \tilde{F}_{k-1}^*(t_{\frac{1}{2}}) \end{bmatrix} \tag{2.25}$$

At time t = $\tau/2$ the RF pulse with flip angle α and phase Φ = 0 is applied to the system and can be described by the following matrix operation:

for all k:

$$\begin{bmatrix} \tilde{F}_k(t_{\frac{1}{2}}) \\ \tilde{F}_k^*(t_{\frac{1}{2}}) \\ \tilde{Z}_k(t_{\frac{1}{2}}) \end{bmatrix}^+ = \begin{bmatrix} cos^2\frac{\alpha}{2} & -sin^2\frac{\alpha}{2} & -i\ sin\alpha \\ sin^2\frac{\alpha}{2} & cos^2\frac{\alpha}{2} & i\ sin\alpha \\ -\frac{i}{2}sin\alpha & \frac{i}{2}sin\alpha & cos\alpha \end{bmatrix} \cdot \begin{bmatrix} \tilde{F}_k(t_{\frac{1}{2}}) \\ \tilde{F}_k^*(t_{\frac{1}{2}}) \\ \tilde{Z}_k(t_{\frac{1}{2}}) \end{bmatrix}^- \tag{2.26}$$

The + and - sign indicates the states before and after the RF pulse respectively. The magnetization is still affected by relaxation and dephasing, therefor the operations mentioned in equations 2.21 - 2.25 are applied in the next t=$\tau/2$. At t=τ an echo is formed which coincides with the measurement point of the MRI scanner. The intensity of the MRI signal at t=τ is determined by the value of $\tilde{F}_0(t1)$.

This whole algorithm is repeated for every RF pulse and in the end all the $\tilde{F}_0(t)$ states for which t is an integer correspond to the intensity of the MRI signal at the subsequent echoes.

2.3 Determine T2 values

Since the T2 value of subcutaneous fat is equal to the T2 value of fatty tissue in an affected muscle, with a fitting process using the EPG model the T2 value of subcutaneous fat is determined. This value is used as a fixed parameter in the EPG model to determine the T2 value of water.

2.3.1 T2 of fat

To determine the T2 value of subcutaneous fat, a fit was performed using the previously described EPG model. The function to describe the signal is:

$$S = p(1) * EPG(TEs, fa_{ex} * p(2), fa_{rf} * p(2), T1, p(3)) \tag{2.27}$$

The values of $\tilde{F}_0(t)$ are only relative values, where 1 is the maximum signal. These values are therefore scaled by a factor p(1) to match the MRI signal. TEs is time at which the MRI signal is measured and an echo is formed. Fa$_{ex}$ and fa$_{rf}$ represent the intended flip angle of the excitation and refocusing pulse respectively. To account for different flip angle values, both are multiplied by the same factor p(2). The T1 value of subcutaneous fat is fixed at the literature value of 360 ms [5]. The fit parameter p(3) represents the T2 value of fat.

The inbuilt function lsqcurvefit of Matlab was used to perform the fit, this function handles non-linear data and solves it in the least-square sense. This function was chosen because it can handle bound constraints on the fit parameters, in that way the output can be limited to physical relevant values. As initial guesses the following values where used:

p(1) = intensity of the first echo
p(2) = 0.9
p(3) = 130 ms

The lower and upper boundaries for these parameters were fixed to:

$0 \leq$ p(1) $\leq$ 2* intensity of the second echo
$0 \leq$ p(2) ≤ 1
$0 \leq$ p(3) ≤ 200

Except for the first echo, all echoes are affected by stimulated echo with a higher echo intensity as a result. It is unlikely that the amplitude parameter is higher than twice the intensity of the second echo. Although there is a chance that the real flip angles are bigger than intended, the upper boundary of p(2) is 1, because, with higher values the fit function ends

up in a loop since a flip angle of 179°and 181°lead to the same outcome. The literature values of subcutaneous fat T2 are around 130 ms, therefore it is unlikely that the value will be above 200 ms. If one of the parameters is determined to be equal to one of its boundaries, details of the relevant voxel is stored.

When this fit is performed on all subcutaneous fat voxels, an average fat T2 value can be determined. This value can be used as a fixed parameter to determine the T2 of water in fat infiltrated muscle.

2.3.2 T2 of water

The same EPG model is used to fit the T2 value of water, except for the equation that describes the MRI signal. Since there is fat and water present in the muscle the MRI signal is a combination of the signals from fat and water. Therefore equation 2.28 is used to describe the MRI signal.

$$S = p(1) * EPG(TEs, fa_{ex} * p(2), fa_{rf} * p(2), T1_{fat}, T2_{fat}) + p(3) * EPG(TEs, fa_{ex} * p(2), fa_{rf} * p(2), T1_{water}, p(4)) \quad (2.28)$$

P(1),TEs, fa_{ex}, p(2), fa_{rf}, have the same function as described in equation 2.27. P(3) is the scaling factor for the MRI signal of water. The literature value of $T1_{water}$ is 1420 ms [5]. P(4) is the fit parameter that represents water T2.

As initial guesses the following values were used:

p(1) = intensity of the first echo/2
p(2) = average of $p(2)_{fat}$
p(3) = intensity of the first echo/2
p(4) = 30 ms

The initial guess of p(2) is based on the average value of the fit parameter p(2) determined in section 2.3.1. The lower and upper boundaries for these parameters were fixed to:

$0 \leq$ p(1) $\leq$ 2* intensity of the first echo
$0 \leq$ p(2) ≤ 1
$0 \leq$ p(3) $\leq$ 2* intensity of the first echo
$0 \leq$ p(4) ≤ 160

Because the MRI signal is a combination of the signal of fat and water, the initial guesses of the amplitudes are both halves of the first MRI signal. There is a change that the voxel contains only water or mostly fat, but it

is unlikely that one of the amplitudes will be higher than twice the MRI signal. The initial guess of water T2 is the literature value of 30 ms [5]. The measured increased water T2 of muscle in the literature [4] is not above 160 ms.

Chapter 3

Results

In the fitting process described in chapter 2 the improved EPG model is used, therefore the effect of the adjustment is demonstrated. The results of the EPG fit on subcutaneous fat is compared to an exponential fit on the same data. An magnetic resonance spectroscopy is performed on a healthy subject to validate the outcome of the EPG model.

3.1 Different B1 values

Compared to the original EPG model [9], the improved EPG model can handle different B1 values: intensity of the RF pulse which is directly related to the flip angle. To demonstrate that this adjustment improves the fit results, two fits were performed on the same voxel containing subcutaneous fat (figure 3.1).

The original EPG model results in a straight decaying line. The alternating MRI echo intensities due to the contribution of stimulated echoes are not described by this model. Whereas the improved EPG model does correct for the difference in signal intensity. This indicates that the improved EPG model describes the MRI signal more accurately.

3.2 Subcutaneous fat

The T2 value of subcutaneous fat is equal to the T2 value of fat in muscles and is used to determine the T2 value of water in muscles. In order to find the fat T2 value, a fit was obtained on voxels containing subcutaneous fat. These fits were performed on a dataset of a patient (Becker Muscular Dystrophy, BMD) with a low degree of fat infiltration in the muscle.

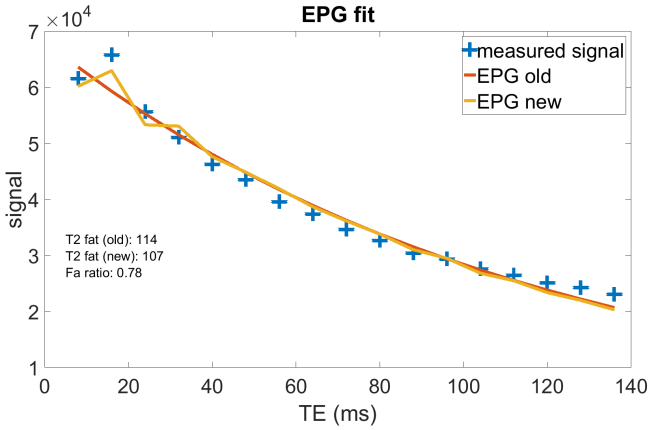

Figure 3.1: *A fit performed on subcutaneous fat using the original EPG model (EPG old) and the improved EPG model (EPG new) where the improved EPG model does correct for different B1 values. The determined T2 value of fat is 114 ms with the original EPG model and 107 ms with the improved EPG model. The ratio between the intended flip angles and the actual flip angles (Fa ratio) is 0.78*

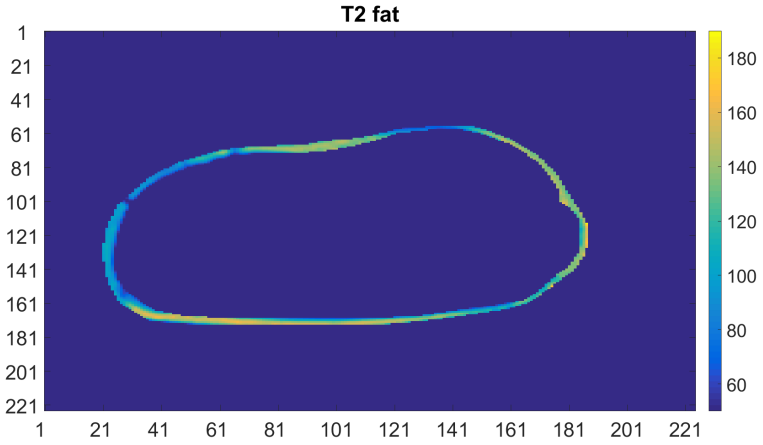

Figure 3.2: *The EPG model was used to determine the T2 value of fat on voxels containing subcutaneous fat. The x- and y-axis represent the location of the voxel in the image.*

Figure 3.2 reveals major differences in the determined T2 values, varies in the range of 100 ms - 160 ms. The question raises regarding the origin of these differences. Are they a consequence of the fitting progress, the data acquisition or are there really these amount of differences among subcutaneous fat. In the last case, it is questionable if one could speak of a single T2 value of fat and if these differences also occur in the T2 value of fatty tissue in the muscles. Because of the assumption that the T2 value of sub-

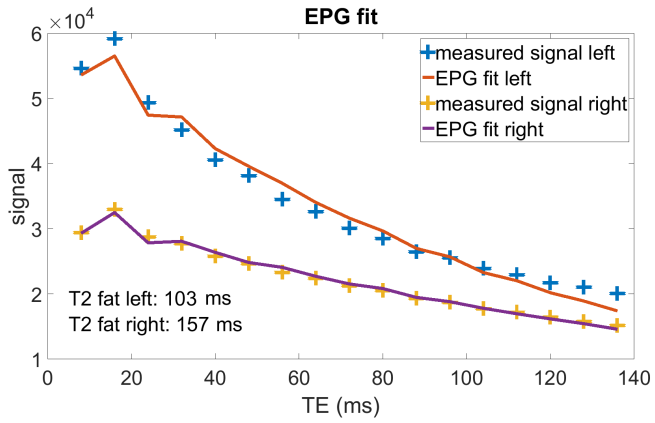

Figure 3.3: *With the EPG model T2 fat values where determined of a voxel on the left and right side of the leg*

cutaneous fat is equal to the T2 value of fat in a muscle, it is necessary to find the origin of these differences before a fixed value of fat T2 is used to determine water T2. The effect of different T2 fat values on the determination of water T2 is demonstrated in table 3.1. The value differences of water T2 when inflammation is present is in the range of several ms (33.7 $\pm$ 2.5 ms for 'normal' water to 38.8 ms and above for 'abnormal' water which can be related to inflammation). As to conclude the influence of the different fat T2 values in fat infiltrated muscles is substantial.

Table 3.1: *Determined values of water T2 using different values of T2 fat in the same muscle voxel of a patient (BMD) with medium degree of fat infiltration.*

T2 fat (ms)	**T2 water (ms)**
100	18
110	21
120	24
130	26
140	27
150	29
160	30

3.2.1 Exponential model

The echo intensity is an exponential process in time, the simplest model to describe the MRI signal is with an exponential decay. To exclude that the

more complicated EPG model causes the differences in T2 fat values, an exponential model was also used on the same data set (Figure 3.4).

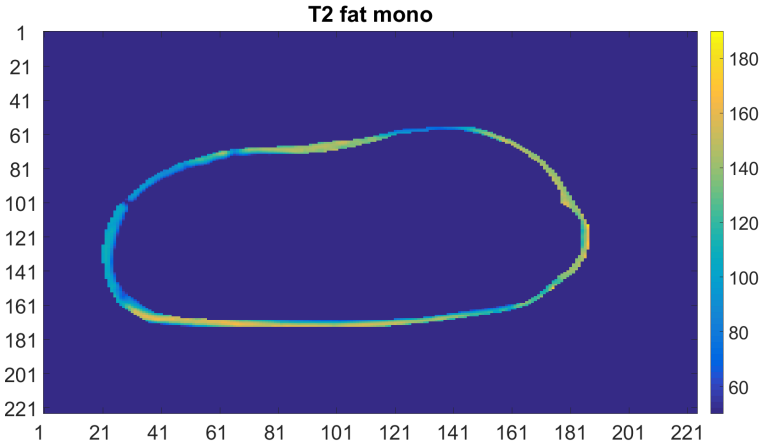

Figure 3.4: *An exponential model was used on all voxels containing subcutaneous fat to obtain the T2 value of fat. The x- and y-axis represents the location of the voxel.*

T2 fat values determined with the EPG model (figure 3.4) shows the same spatial differences as the T2 fat values determined with the exponential model (figure 3.2). The scatter plot (figure 3.5) shows that the T2 fat values determined with the EPG model and the exponential model are well-nigh equal.

3.2.2 MR spectroscopy on a healthy subject

The main differences in T2 values are between the left and right side of the leg. With magnetic resonance spectroscopy (MRS) the fat T2 values of both regions can be obtained. If the more complicated acquisition of MRI causes the differences in T2 values, the MR spectroscopy would show equal T2 fat values. An MR spectroscopy was obtained on the left and right side of the lower leg from a healthy subject as well as an MRI in order to compare the T2 values.

The differences in T2 fat values of the healthy subject (figure 3.6) are smaller compared to the T2 fat values of the patient (figure 3.2) as can be seen in table 3.2. The MRS confirms a difference (figure 3.7), but these values are lower than the values determined by the EPG model and the highest value obtained with MRS is at a different side of the leg than the high values obtained with the EPG model.

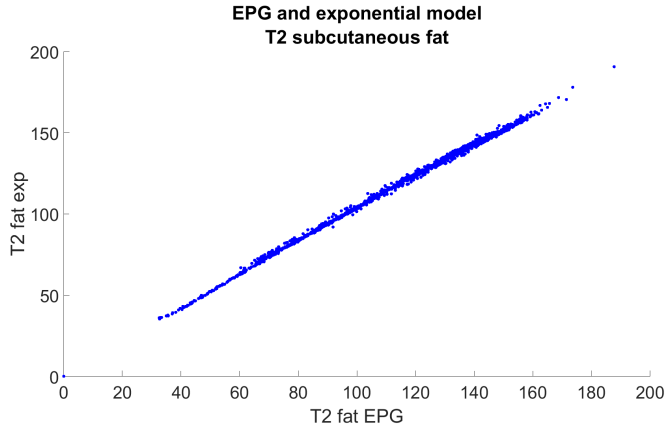

Figure 3.5: *Scatter plot of T2 fat values determined with the EPG model against the exponential model. The linear correlation between the two values suggests that the spatial differences in T2 fat values is independent of the complexity of the model.*

Table 3.2: *Differences in T2 values of subcutaneous fat between left and right. Obtained using the EPG model and MRS.*

subject	T2 fat left (ms)	T2 fat right (ms)
patient EPG	100	160
healthy EPG	143	120
healthy MRS	61	73

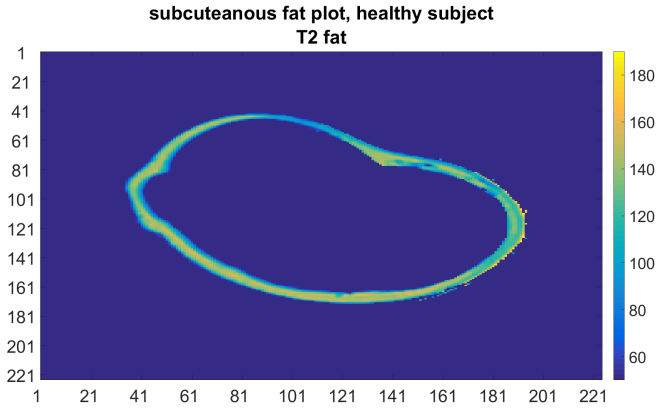

Figure 3.6: *An EPG model was used on all voxels containing subcutaneous fat of a healthy subject to obtain the T2 value of fat. The x- and y-axis represent the location of the voxel.*

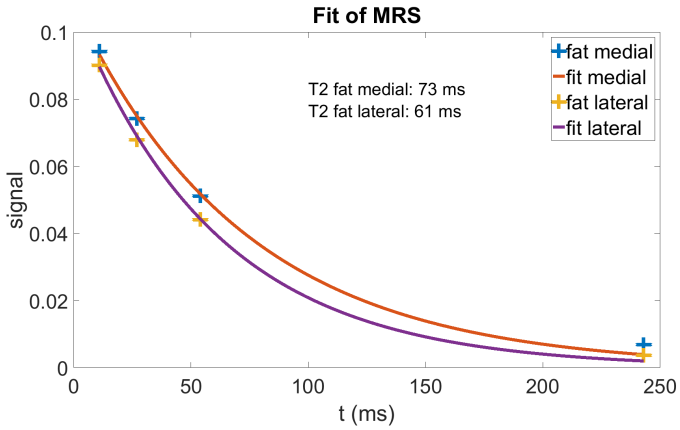

Figure 3.7: *Magnetic resonance spectroscopy performed on a voxel at the left (lateral) and on the right (medial)*

Chapter 4

Discussion

Three problems arise from the results. Firstly, the T2 fat values between left and right side of the leg determined with the EPG model differs 60 ms in the patient's data compared to 20 ms in the data obtained on a healthy subject. A possible explanation could be insufficient shimming during acquisition. Secondly, the determined T2 fat values with the EPG model differs from the obtained values with MR spectroscopy. Several probabilities for this problem are explored where dephasing in the EPG model, water fat shift and slice profile of the RF pulse remain as possible causes. Finally, the T2 fat values obtained with MR spectroscopy and the EPG model show different values for the left and right side of the leg. No clear explanation could be found for these differences.

4.1 Different T2 values of patients subcutaneous fat

An unexpected outcome was the spatial differences in determined T2 values of subcutaneous fat. These differences were between left and right side of the leg and even between three subsequent voxels (figure 4.1). MR spectroscopy could confirm if the differences between left and right are real. A voxel of MRS is larger than of MRI, therefore, it would only be possible to examine the spatial differences between areas of the leg and not between subsequent voxels. No MRS data was available of the patient, therefore an MRI and MRS were obtained of a healthy subject assuming that subcutaneous fat is unaffected by the muscular dystrophy disease.

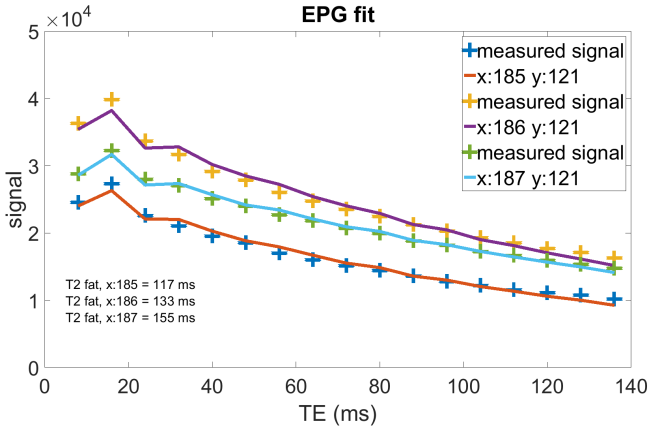

Figure 4.1: *The EPG model was used to determine the T2 fat values of three subsequent voxels (horizontal direction) containing subcutaneous fat. The T2 fat values are remarkably different.*

4.1.1 MRI acquisition

The MRI (figure 3.6) and MRS (figure 3.7) on the healthy subject show spatial differences but to a lesser extent. Which excludes the option that these differences of 60 ms are physiological but does not explain why they appear in imaging. The same MRI acquisition was used to obtain the data of the patient and the healthy subject but since the difference in T2 values is less for the healthy subject it is unlikely that the MRI acquisition causes the differences of 60 ms in the data of the patient.

4.1.2 Shimming

A reason that the differences between T2 values of the patient (figure 3.2) are three times higher than of the healthy person (figure 3.6), could be imperfections during scanning. Shim coils are tuned to correct for an imperfect B_0 field, when this did not happen successfully during the scan of the patient, the data could be less accurate. In that case, the phase data of the signal would reveal this by remarkable differences in phase. Phase data of the patient MRI is unfortunately unavailable.

4.2 Improvement of the EPG model

The EPG model is adjusted so it can handle excitation pulses, but since there is a basis transformation from complex to Fourier space it is ques-

tionable if it is the right adjustment. The result of a 90°excitation pulse around the y-axis as seen from the complex plane is that the magnetization vector resides on the x-axis, therefor:

$$M_+ = 1 \tag{4.1}$$
$$M_- = 1 \tag{4.2}$$
$$M_z = 0 \tag{4.3}$$

Since an arbitrary excitation pulse α only influences the x and z value of M, it can be described by:

$$M_+ = sin(\alpha) \tag{4.4}$$
$$M_- = sin(\alpha) \tag{4.5}$$
$$M_z = cos(\alpha) \tag{4.6}$$

According to the article [9] a 90°excitation pulse has a result on the magnetization in Fourier space to be:

$$\tilde{F}_0 = 1 \tag{4.7}$$
$$\tilde{F}_0^* = 1 \tag{4.8}$$
$$\tilde{Z}_0 = 0 \tag{4.9}$$

It would therefor be reasonable to describe an arbitrary excitation pulse α by:

$$\tilde{F}_0 = sin(\alpha) \tag{4.10}$$
$$\tilde{F}_0^* = sin(\alpha) \tag{4.11}$$
$$\tilde{Z}_0 = cos(\alpha) \tag{4.12}$$

Is this the correct way to handle the magnetization in this basis transformation? The definition of $\tilde{F}_k$ is [9]:

$$\tilde{F}_+(k) = \int_V M_+(r) e^{-ikr} d^3r \tag{4.13}$$

with $M_+(r)$:

$$M_+(r) = Mcos(kr) \tag{4.14}$$

Where M is the magnitude of the group of spins, in the case of an arbitrary excitation pulse α: $M = sin(\alpha)$. M does not depend on r and the Fourier transform is linear therefor the magnetization can be described by equations 4.10- 4.12.

4.3 Initial guesses

The initial guesses of the amplitudes of fat and water stated in section 2.3.2 are both halves of the intensity of the first echo. In the cases of low to medium degree of fat infiltration, these initial guesses have no influence on the determination of T2 water. However, this guess is less sufficient when there is a lot of fat present in the voxel. In that case, the fit is not able to find a solution, if the initial guesses are changed to a fat-water ratio of 1:0, the fit converges to a solution. But then, most T2 water values are determined to be equal to the upper boundary and therefore unreliable.

4.4 Dependence of the parameters

If values of T2 fat depends on the other fit parameters a scatter plot would display this relationship. Ideally, no dependency exists. In figure 4.2 (a) the determined T2 values are plotted against the determined Fa ratios (ratio between intended and actual flip angle). For T2 values up to 60 ms, the Fa ratio corresponds in a linear way. But for higher values, there is no correlation. A scatter plot between amplitudes (A fat) and T2 fat values (figure 4.2 (b)) shows a small correlation for T2 fat values lower than 100 ms and no dependency for higher T2 values. The small correlation between T2 fat and the other parameters is not a clear explanation for the differences in T2 values determined with the EPG model.

4.5 Noise level

In theory, the intensity of the MRI signal decays to zero, in practice, the signal is affected by noise and decays up to a noise level. The function to describe the MRI signal (equation: 2.27) could be improved by taking the noise level into account (equation: 4.15).

$$S = A * EPG(TEs, fa_{ex} * B1, fa_{rf} * B1, T1, T2) \; + \; \delta \qquad (4.15)$$

The amplitude of the signal is describe by: A, TEs is time at which the MRI signal is measured and an echo is formed. Fa$_{ex}$ and fa$_{rf}$ represent the intended flip angle of the excitation and refocusing pulse respectively, both are multiplied by the same factor B1, in order to account for different values of the flip angles. T1 and T2 are the relaxation times of the signal and δ represents the noise level.

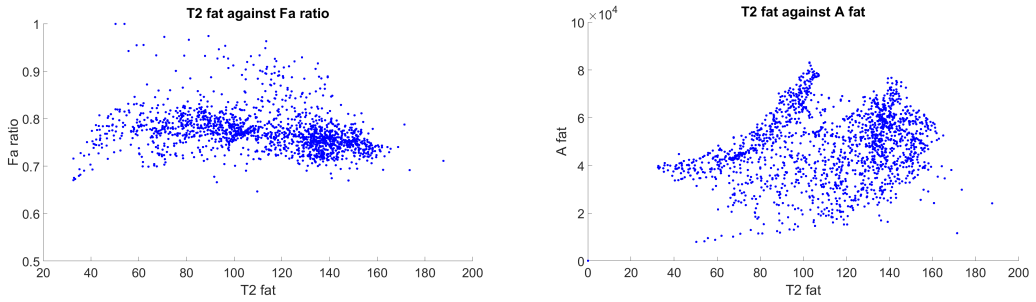

(a) T2 against Fa ratio

(b) T2 against amplitude

Figure 4.2: *a) A scatter plot between the determined T2 value of subcutaneous fat and the FA ratio. There is a small linear correlation between T2 values lower than 60 ms, but for higher values there is no correlation. b) A scatter plot between the determined T2 value of subcutaneous fat the amplitude determined with the EPG model. A small dependency exists for T2 values up to 100 ms since the T2 values increase together with the amplitude value. There is no correlation for T2 values higher than 100 ms.*

The signal intensities are not comparable between scans and as a result, it is not possible to add a fixed parameter to equation 4.15 when this noise level is not explicitly measured for each scan. But a fit parameter could be added to fit this noise level. With this extra parameter, it fits the MRI signal more precise (figure 4.3).

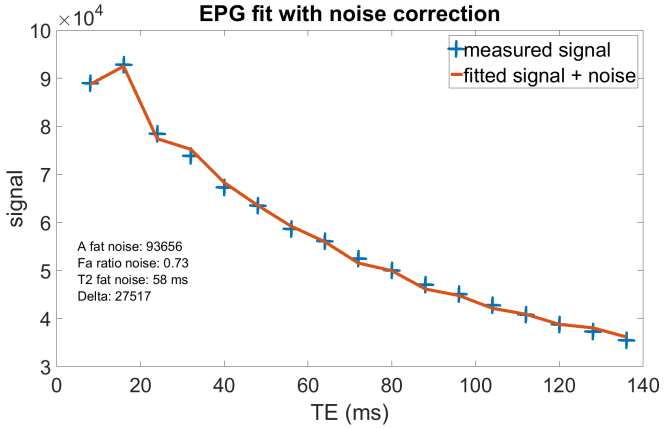

Figure 4.3: *The EPG model is used to perform a fit on a voxel containing subcutaneous fat. An extra variable is added to account for the noise level.*

On the other hand, the fitted value for the noise level is a quarter of the highest measured signal, which is unlikely. Therefore it seems that adding

the noise fit parameter results in a better fit because it is an extra degree of freedom rather than that it is a more accurate description of the reality.

If the obtained T2 fat value depends on the noise level a relation exists between T2 fat and echo intensity since low signal intensities are related to higher noise. The scatter plot (figure 4.4) between T2 fat and the intensity of the second echo shows a small correlation of T2 values up to 100 ms, were the T2 value increases together with the intensity. But for T2 values higher than 100 ms there seems to be no dependency.

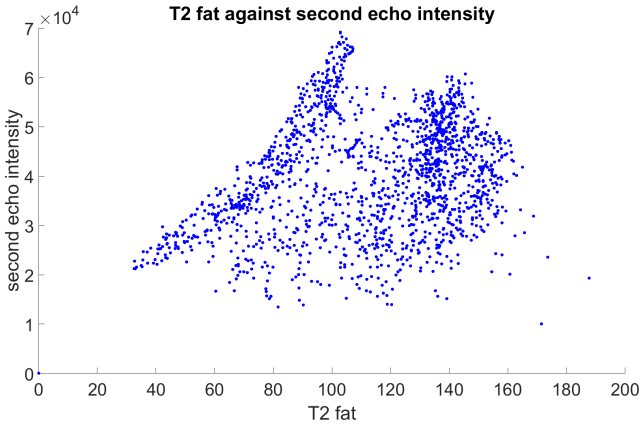

Figure 4.4: *The EPG model is used to obtain the T2 fat value. This scatter plot displays the T2 fat value against the second echo intensity.*

4.6 Dephasing in the EPG model

The slice gradient, applied during the RF pulses, causes the spins to rotate at different frequencies and as a result, the spins dephase relative to each other. The EPG model describes this dephasing with the coordinate k. When the phase difference of the magnetization of a group of spins is increasing the relative difference in k will increase as well. Every time the magnetization in the EPG model dephases (equations 2.24 and 2.25), k is shifted by Δk. The gradients used during the 90°and 180° RF pulses are slightly different, 1.78 mT/m and 1.81 mT/m respectively, resulting in different dephasing rates. The EPG model does not count for this difference and uses $\Delta k = 1$ regardless of the gradient strength. The same problem emerges when EPG is used to model the MRI signal of a fat infiltrated muscle, where the signal is a combination of fat and water. The resonate frequency of water and fat differ, causing them to dephase at a different rates relative to each other. Therefore, ΔK in the EPG model should be

different for fat and water, but it is not clear how the value of Δk is related to actual dephasing rates and gradient strengths.

4.7 Water fat shift

The determined T2 fat values with the EPG model differ from the real T2 fat values obtained with MR spectroscopy, suggesting inaccuracy of the EPG model. Since the difference appears in the frequency-encode direction, it could be caused by a chemical shift artefact. The shielding effect mentioned in section 1.1.4 causes the spins of fat to resonate at a different frequency than spins of water. Only one frequency can be used to determine the location of the spins, in this measurement this frequency is set equal to the resonate frequency of water. As a result, the signal from fat will be seen by the system as a signal from water that resides in a voxel further away [13]. The subcutaneous fat voxels on the right side contain only signals from fat, but the subcutaneous fat voxels on the left side of the leg are mapped to the same spot as water. To model these voxels on the left side of the leg accurately another term should be added to account for the water signal.

4.8 Slice profile

A different slice profile could be another explanation for the discrepancy between the real T2 fat values and determined values with the EPG model. The improved EPG model can account for different B1 values, but on average the ratio between the intended and real flip angle (FA ratio) is 0.75. The reason for this low determined FA ratio is to compensate for the difference of the echo intensities between the first and the other echoes. Except for the first echo, all echo intensities are affected by stimulated echoes. Due to the RF pulse, part of the magnetization is placed in the z-direction and contributes as a stimulate echo in a later echo to its intensity. This process is not present until the second echo, therefore the intensity of the first echo is always lower than the second [14]. The impact of stimulated echoes to the signal intensities increases for smaller flip angles [15] which explains the FA ratio of 75%. But the expected efficiency rate of the real flip angle is estimated to be up to 90%.

The pulse profile could explain that the estimated FA ratio is lower than expected. It is assumed that all spins in the MRI slice are flipped with the same angle. When a certain pulse profile (sinc wave or Gaussian-shaped)

is applied, all spins will flip. But the spins resonate at different frequencies and therefore the flip angle due to the pulse will differ along the slice. The MRI signal intensity, therefore, depends on the position of the spins. The measured intensity is a sum of all intensities along the slice. Since some of the spins will be flipped by a lower flip angle their stimulated echo contribution will be higher. By implementing this pulse profile it should be possible to simulate the high contribution of stimulated echoes without underestimating the overall flip angle.

Once this effect is implemented in the EPG model, the chemical shift could prevent accurate determination of values. The settings of the RF pulse, (duration, intensity, profile) is tuned to flip the water spins in the specific slice. As mentioned in section 4.7 the frequency of the fat spins are different from water spins, the RF pulse, therefore, has a different effect on the fat spins.

4.9 T2 fat value of left and right side

The table showing the T2 fat values determined with the EPG model and with MRS (table: 3.2) of the healthy subject reveals two unexpected results. First, the higher T2 fat values obtained with the EPG model are determined on the other side of the leg than the higher T2 fat values obtained with MRS. This discrepancy could be solved if the improvements mentioned above are implemented in the EPG model since the subcutaneous fat voxels on the left side of the leg are affected by the water fat shift, whereas the MRS data is not affected by this chemical shift. Although, the MRI of the patient was obtained from the right leg, whereas the healthy subject's left leg was imaged. As a result, the higher T2 fat values where obtained at the outside (lateral) of the leg and the lower values at the inside (medial), suggesting that another factor is related to this problem.

The MRS shows unexpected different T2 fat values between the left and right side of leg The MRS acquisition uses the different frequencies of water and fat to distinguish the signals between both molecules, in other words, MRS is not affected by chemical shift artefacts and cannot cause these differences. The MRS data was acquired twice on the same spot, difference in determined T2 fat values between the two dataset indicates the effect of noise. Since this effect is $\pm$ 1 ms it cannot cause the difference of 10 ms. Biological or chemical dissimilarities could explain the differences, but this unlikely since the same sort of fat is expected around the lower leg. Which is also the reason why similar values were expected. Therefore it is not clear why differences of 10 ms appear in the MRS data.

Chapter 5

Conclusion

T2 of water increases when inflammation is present in the muscle. When the muscle is infiltrated by fat, the MRI signal needs to be separated into water and fat signal. The T2 of water can be determined by using a model, where the T2 of fat is a fixed value. MRI signal from subcutaneous fat is used to determine T2 fat since it is equal to T2 of fatty tissue in the muscle. The obtained T2 water value is influenced by the value of T2 fat and the degree of fat infiltration. The determined T2 water value is unreliable in severe fat infiltrated muscles.

Previously used exponential models to determine the T2 fat value do not account for stimulated echoes in the MRI signal, whereas the Extended Phase Graph algorithm can calculate the contribution of these stimulated echoes to the signal.

The difference in T2 fat values obtained from the left and right side of a patient's (BMD) leg was 60 ms. The EPG model was not causing this difference since the simpler exponential model showed the same amount of difference. The same MRI acquisition was used to obtain data of a healthy subject, revealing differences of only 20 ms. A possible explanation of the 60 ms differences is an inefficient shimming process.

With MR spectroscopy T2 fat values were measured on the left and right side of a healthy subject, which were different from the values obtained with the EPG model, suggesting imperfections of the model.

The EPG model was improved correctly to handle different values of the RF pulses, the determined values do not depend on the chosen initial guesses, the parameters are not much correlated to each other and T2 fat values do not depend on noise. Possible imperfections of the model include the dephasing rates which are assumed to be the same for all gradient strengths and resonant frequencies. The water fat shift causes the

subcutaneous fat voxels on the left side of the leg to be mapped onto the muscle voxels, this could be corrected by including the water signal in the model. Another unrealistic assumption was the shape of the RF pulse to be a block wave, causing all the spins in the slide to flip by the same flip angle. A variation of flip angles along the slice should improve the model.

When accurate T2 fat values can be obtained the chemical shift could obstruct an accurate determination of water T2. However, this won't solve the fact that the T2 fat value differs in the order of 10 ms along subcutaneous fat, which influences the determination of water T2 in fat infiltrated muscles. The high T2 fat values obtained with the EPG model seem to be located lateral, whereas the low T2 fat values seem to be located medial, which is opposite to the determined values with MR spectroscopy. These remarkable outcomes request for further research.

Acknowledgement

I would like to offer my special thanks to dr. J.W.M. Beenakker for his outstanding supervision and guidance during my bachelor project, especially for his patience during explanations. I am particularly grateful for the support given by Dr. H.E. Kan and all members of the C.J. Gorter center for their help and kindness.

Bibliography

[1] M. T. Hooijmans, E. H. Niks, J. Burakiewicz, J. J. Verschuuren, A. G. Webb, and H. E. Kan, "Elevated phosphodiester and T2 levels can be measured in the absence of fat infiltration in Duchenne muscular dystrophy patients," *NMR in Biomedicine*, vol. 30, no. 1, 2017.

[2] J. Burakiewicz, C. D. Sinclair, D. Fischer, G. A. Walter, H. E. Kan, and K. G. Hollingsworth, "Quantifying fat replacement of muscle by quantitative MRI in muscular dystrophy," *Journal of Neurology*, pp. 1–15, 2017.

[3] C. M. Mcdonald, E. K. Henricson, R. T. Abresch, J. M. Florence, M. Eagle, E. Gappmaier, A. M. Glanzman, R. Spiegel, J. Barth, G. Elfring, A. Reha, and S. Peltz, "THE 6 minute walk test and other endpoints in Duchenne muscular dystrophy: Longitudinal natural history observations over 48 weeks from a multicenter study," *Muscle and Nerve*, vol. 48, no. 3, pp. 343–356, 2013.

[4] N. Azzabou, P. L. De Sousa, E. Caldas, and P. G. Carlier, "Validation of a generic approach to muscle water T2 determination at 3T in fat infiltrated skeletal muscle," *Journal of Magnetic Resonance Imaging*, vol. 41, no. 3, pp. 645–653, 2015.

[5] N. Smith and A. Webb, *Introduction to medical imaging: physics, engineering, and clinical applications*. 2011.

[6] D. Weishaupt, V. D. Köchli, and B. Marincek, *How does MRI work?* 2008.

[7] X. J. Bernstein, Matt A.; King, Kevin Franklin.; Zhou, "echo train pulse sequences," in *Handbook of MRI pulse sequences*, pp. 796–835, 2004.

[8] A. D. Elstar, "Fat/Water Chemical Shift," 2017.

[9] M. Weigel, "Extended phase graphs: Dephasing, RF pulses, and echoes - Pure and simple," *Journal of Magnetic Resonance Imaging*, vol. 41, no. 2, pp. 266–295, 2015.

[10] The MathWorks, *MATLAB and Statistics Toolbox*. Inc., Natick, Massachusetts, United States, 2016. ISBN 3-900051-07-0.

[11] R. Kaiser, E. Bartholdi, and R. R. Ernst, "Diffusion and field gradient effects in NMR Fourier spectroscopy," *The Journal of Chemical Physics*, vol. 60, no. 8, pp. 2966–2979, 1974.

[12] J. Wang, W. Mao, M. Qiu, M. B. Smith, and R. T. Constable, "Factors influencing flip angle mapping in MRI: RF pulse shape, slice-select gradients, off-resonance excitation, and B0 inhomogeneities," *Magnetic Resonance in Medicine*, vol. 56, no. 2, pp. 463–468, 2006.

[13] A. D. Elstar, "Chemical Shift Artifact," 2017.

[14] M. N. Uddin, R. Marc Lebel, and A. H. Wilman, "Transverse relaxometry with reduced echo train lengths via stimulated echo compensation," *Magnetic Resonance in Medicine*, vol. 70, no. 5, pp. 1340–1346, 2013.

[15] J. Hennig, "Multiecho imaging sequences with low refocusing flip angles," *Journal of Magnetic Resonance (1969)*, 1988.